JOURNAL OF
Materials
CHEMISTRY

Probing the surface acidity of lithium aluminium and magnesium aluminium layered double hydroxides

Ian C. Chisem,[a] **William Jones,**[a*†] **Ines Martín,**[b] **Cristina Martín**[b] **and Vicente Rives**[b]

[a]*Department of Chemistry, University of Cambridge, Lensfield Road, Cambridge, UK CB2 1EW*
[b]*Departamento de Quimica Inorganica, Universidad de Salamanca, Salamanca, Spain*

The surface acidity of a range of lithium aluminium layered double hydroxides intercalated with carbonate, chloride, nitrate and decavanadate anions has been measured using Hammett indicators. In addition, the adsorption of pyridine and isopropanol has been monitored using infrared spectroscopy. The properties of the materials have been compared to their magnesium aluminium analogues. Surface measurements are compared with the observed catalytic activity for acetaldehyde self-condensation and 2-methylbut-3-yn-2-ol conversion. The MgAl matrix was found to be more stable than the LiAl matrix following calcination at the elevated temperatures which yielded the most active catalysts (*ca.* 450 °C). The order of acidity of the materials varied with the nature of the anion such that: carbonate < nitrate < chloride < decavanadate. Thus it was concluded that the nature of the interlayer anion had a large effect on the acidity of the materials, although the acidity was largely unaffected by the identity of the host matrix itself.

Introduction

Layered double hydroxides (LDHs) are mixed metal hydroxides of the general formula $[M^{z+}{}_{1-x}M^{3+}{}_{x}(OH)_2]^{a+}[X^{m-}]_{a/m}\cdot nH_2O$ where $a=x$ when $z=2$, and $a=2x-1$ when $z=1$. The positively charged hydroxide layers $[M^{z+}{}_{1-x}M^{3+}{}_{x}(OH)_2]^{a+}$ are charge-balanced by the presence of interlayer anions $[X^{m-}]_{a/m}$. By modification of parameters such as the $M^{I/II}:M^{III}$ ratio, calcination temperature and the interlayer anion it is possible to influence the strength and number of catalytically active sites of a LDH in order to tailor the catalyst for a specific reaction. Furthermore, by exchange of the interlayer anion the acidity or basicity of the accessible catalytic sites may be altered. Solid acid catalysts have been used in many industrial processes such as catalytic cracking, organic synthesis, alkylation and isomerization reactions.[1–4] Basic catalysts have fewer applications but still there is great interest in their characterisation.[5–8] Although this field is still largely unexplored, there are many possibilities for catalysing the production of fine chemicals and commodities.[9–12] LDHs have been used as precursors to catalysts for the polymerisation of alkene oxides and for aldol condensations. Vanadate-intercalated LDHs have a possible application as precursors to catalysts for the selective oxidation of short chain paraffins in order to synthesise valuable organic chemicals. A comprehensive review of their other catalytic applications was provided by Cavani *et al.*[13]

The vast majority of the catalytic studies regarding LDHs concern the hydrotalcite-like materials $[Mg_6Al_2(OH)_{16}CO_3\cdot nH_2O]$, and there is no widespread study of the catalytic properties of the corresponding lithium aluminium system. In this paper, the catalytic activities of both magnesium aluminium and lithium aluminium LDHs containing carbonate, chloride, nitrate and vanadate are studied, both before and after calcination at a range of temperatures. We report on the effect of varying the cationic matrix and the nature of the interlayer anion on the catalytic activity for reactions catalysed by either Lewis or Brønsted acid or basic sites and, in particular, two reactions are investigated: (i) acetaldehyde self-condensation and (ii) 2-methylbut-3-yn-2-ol dehydrogenation/cleavage. We also report on the determination of the number and type of acid/base sites using the adsorption of the probe molecules pyridine and isopropanol on the surface of the LDH catalysts.[14–16] Surface acidity is further probed using Hammett indicators.

Experimental section

Catalyst preparation

Most reagents were ACS reagent grade from the Aldrich Chemical Company Ltd. or Fisons plc. N_2 gas was obtained from Distillers MG. Water was decarbonated (by distillation) and deionised. Samples after synthesis were dried in air at 100 °C for 18 h.

In the case of MgAl LDHs, the materials were prepared with a Mg : Al ratio of 2 : 1. LiAl LDHs were prepared with a Li : Al ratio of 1 : 2. Henceforth, the materials will be described in the form $M^{I/II}M^{III}X$, such that a material of structural formula $Mg_4Al_2(OH)_{12}CO_3\cdot nH_2O$ is represented as $MgAlCO_3$, and a material of composition $LiAl_2(OH)_6Cl\cdot nH_2O$ is represented as LiAlCl.

$LiAlCO_3$ was prepared by a method described previously by Chisem and Jones.[17] $MgAlCO_3$ and MgAlCl were prepared by coprecipitation reactions according to the procedure of Constantino and Pinnavaia.[18]

$LiAlNO_3$ and $MgAlNO_3$ were prepared by anion exchange of the parent carbonate-intercalated derivative in acid media. $MgAlCO_3$ or $LiAlCO_3$ (1.0 g) was added to 150 ml water and the pH was adjusted to 4.5 by the addition of 0.1 M HNO_3. The addition was accompanied by rapid expulsion of CO_2. The mixture was stirred whilst maintaining the pH at 4.5 by further addition of acid. The reaction was carried out at room temperature for 72 h to produce $LiAlNO_3$ or 5 h to produce $MgAlNO_3$. The resulting products were isolated by filtration or centrifugation and washed several times with water. LiAlCl was prepared by a similar method, although HCl was the acid used to promote the exchange, and the reaction was carried out for a period of 24 h at room temperature.

The vanadate intercalates were prepared by the following method: a 150 ml solution of 0.1 M $NaVO_3$ was adjusted to pH 4.5 by addition of 0.5 M HCl. $MgAlCO_3$ or $LiAlCO_3$ (1.0 g) was added and the pH adjusted to 4.5 by addition of 0.1 M HCl. The mixture was stirred at room temperature and the pH was maintained at 4.5 throughout the course of the reaction by further addition of 0.1 M HCl. The reaction was carried out

---

† E-mail: wj10@cus.cam.ac.uk

for a period of 5 h. The resulting product was isolated by filtration or centrifugation and washed with water.

Catalyst characterisation

X-Ray diffraction measurements were performed using a Philips PW 1050 goniometer, with a PW 1710 control unit. A graphite monochromator and Cu-Kα radiation ($\lambda = 1.5418$ Å) were used, with a Ni filter for Kβ attenuation. Randomly oriented samples on glass slides were used to obtain the patterns. Samples were scanned from 3–80° (2θ) with a step scan of 0.05° (2θ) at a rate of 0.05 s^{-1}.

Infrared spectra were recorded at room temperature using a Nicolet 205 Fourier transform infrared spectrometer. The sample was mixed with infrared grade KBr and pressed to form a disc, and then analysed from 4000 to 400 cm^{-1}, with a resolution of 2 cm^{-1} and 60 scans averaged.

The weight loss on heating samples from 25–800 °C at a rate of 10 °C min^{-1} under a nitrogen flow (25 ml min^{-1}) was determined using a Polymer Laboratories TGA1500 thermogravimetric analyser.

Combined thermogravimetric analysis and mass spectrometry was performed using a Leda-Mass Mini Lab mass spectrometer linked to a Polymer Laboratories TGA 1500 by a quartz capillary transfer line heated to 120 °C.[19] Samples were heated from 25 to 800 or 1200 °C at a heating rate of 30 °C min^{-1} under a nitrogen flow (25 ml min^{-1}). The TGA apparatus was at atmospheric pressure, and the mass spectrometer had a working pressure of 6×10^{-7} Torr and an electron energy of 70 eV.

Elemental chemical analysis for magnesium, lithium, aluminium and vanadium was performed using a Perkin Elmer Atomic Absorption Spectrometer 3100. Carbon, hydrogen and nitrogen were determined using a Perkin Elmer 2400C instrument.

Infrared studies of adsorbed pyridine and isopropanol

The surface acidity was investigated by adsorption of pyridine and isopropanol on self-supporting discs. FTIR spectra of adsorbed species were recorded on a Perkin Elmer 16PC (University of Salamanca) or a Nicolet 205 spectrometer (University of Cambridge). The self-supported disc (wafer concentration 10–20 mg cm^{-2}) was placed in a specially designed vacuum glass cell in order to perform thermal treatments and adsorption of gases and vapours *in situ*.

Adsorption of pyridine and isopropanol was studied in the FTIR vacuum cell following *in situ* calcination of the sample for 2 h in air (at temperatures of 250 °C or 400 °C) and outgassing at *ca.* 10^{-3} Torr for 2 h to withdraw species adsorbed during manipulation of the sample. The gaseous pyridine or isopropanol was then adsorbed on the surface of the sample, which was then outgassed at increasing temperatures at 10^{-3} Torr. The infrared measurements were made at room temperature. The background of the clean degassed sample was subtracted under software control in each case so that only the bands of the adsorbed probe molecules were evident.

Hammett indicator tests

In order to determine the maximum acid strength of the materials 2 ml of the indicator, dissolved in benzene or dichloromethane, was added to 0.2 g of a finely powdered sample, shaken briefly and the colour change noted.

Catalytic studies

Acetaldehyde condensation was carried out using a batch catalysis method. The catalysts used in the study were calcined in air for 2 h at 200, 400 or 600 °C prior to reaction. The reactant (3.0 ml) was added to 0.3 g solid LDH catalyst in a (non-stirred) stainless steel pressure vessel and reacted for 5.5 h at 110 °C. The reaction was then quenched by plunging the reaction vessels into ice. After cooling the liquid product was decanted and the product ratios were analysed using a Carlo Erba HRGC 5300 gas chromatograph.

2-Methylbut-3-yn-2-ol (MBOH) conversion was carried out using a pulse microreactor with a helium flow of 25 ml min^{-1}. The catalyst bed (0.05 g; 30–60 mesh) was activated for 2 h at 450 °C. The volume of one MBOH pulse was 1.0 µl. Products were separated and analysed using a Carlo Erba HRGC 5300 gas chromatograph on line with the microreactor.

Results and Discussion

Catalyst characterisation

A. Carbonates. Characterisation of carbonate intercalated LDHs has been discussed in detail elsewhere.[17,20–23] Powder X-ray diffraction of both $MgAlCO_3$ and $LiAlCO_3$ shows the materials to have a layer repeat distance of *ca.* 7.6 Å, corresponding to an interlayer spacing of *ca.* 2.8 Å. FTIR spectroscopy shows bands of D_{3h} carbonate anions at 875 and 665 cm^{-1}, and the ν_3 band of the carbonate anion at 1365 cm^{-1}. In addition, a shoulder at *ca.* 3050 cm^{-1} may be attributed to hydrogen bonding between the interlayer carbonate and water. As expected, chemical analysis shows the Al : Li and Mg : Al ratios for $LiAlCO_3$ and $MgAlCO_3$ respectively to be close to two. The most striking difference between these two materials lies in their thermal stabilities, with layer dehydroxylation occurring at much higher temperatures for $MgAlCO_3$ than for $LiAlCO_3$. The carbonate anion is also more stable in the $MgAlCO_3$ than the corresponding LiAl compound. Hernandez *et al.*[24] noted that the thermal stability of lithium hydrotalcite is quite different from other compounds with an LDH structure.[20,21,25–27] In Ni or Mg analogues with a $M^{II}:M^{III}$ ratio of 2, interlayer water is lost between 200 and 300 °C but the hydrotalcite-like structure is retained. The layered structure is preserved up to temperatures of 350–500 °C. For $LiAlCO_3$ decomposition occurs at temperatures below 240 °C. Hernandez *et al*[24] proposed that lithium hydrotalcite decomposed to form γ-$LiAlO_2$ and $LiAl_5O_8$ over a wide range of temperatures between 200 and 1000 °C.

B. Chlorides. The PXRD patterns of MgAlCl and LiAlCl show these materials to have an interlayer repeat distance of *ca.* 7.5 Å, which is similar to that of the carbonate derivatives, although the absence of bands due to carbonate in the FTIR spectrum suggests that complete exchange of carbonate for chloride has indeed been achieved.

Once again, there are interesting differences in the thermal properties of the two materials. TG-MS measurements show MgAlCl to be stable up to *ca.* 300 °C: below this temperature, the material releases water at temperatures between 50 and 280 °C. This has been attributed to two different types of water;[18] surface water, which is lost between 50 and 150 °C, and interlayer water, lost between 150 and 280 °C. Miyata[21] attributed an endothermic DTA peak at 230 °C to the liberation of interlayer water. Above the decomposition temperature of *ca.* 300 °C, the TG/DTG curve for MgAlCl shows two weight loss steps; one between 300 and 380 °C and the other at 380–580 °C. According to earlier workers,[21,28] the first step involves the liberation of water through dehydroxylation processes and the second step is attributed to the release of Cl^- ions as HCl.

The thermal behaviour of LiAlCl is markedly different, however. Three distinct weight losses are seen, centred at *ca.* 80, 275 and 330 °C. These correspond to loss of surface water, interlamellar water and dehydroxylation respectively. The chloride species is, in this case, stable up to 800 °C. This could be explained in terms of the grafting of chloride groups onto the layers themselves, replacing hydroxyl groups. A similar mechanism has been used to explain the high acidity of fluorinated cationic clays,[29] and Constantino and Pinnavaia[18] have explained the catalytic selectivity of MgAlCl LDH in terms of this behaviour.

C. Nitrates. $MgAlNO_3$ and $LiAlNO_3$ both exhibit expanded layer repeat distances of *ca.* 8.8 Å. The materials exhibit a strong band at *ca.* 1385 cm^{-1} in the FTIR spectrum attributed to the ν_3 band of NO_3^-, and a weak ν_2 band at *ca.* 825 cm^{-1} as observed by Hernandez-Moreno *et al.*[30] In terms of thermal stability, $MgAlNO_3$ exhibits a gradual weight loss up to 600 °C indicating that dehydroxylation and nitrate decomposition occur over a wide temperature range. In contrast, three sharp and distinct transitions are observed for the LiAl material, corresponding to loss of interlamellar water, dehydroxylation and nitrate loss, in order of increasing temperature. $LiAlNO_3$ is stable up to a temperature of *ca.* 250 °C, at which dehydroxylation processes occur.

D. Vanadates. MgAlV and LiAlV have identical interlayer spacings of *ca.* 6.8 Å. This, and elemental analysis data, suggests that decavanadate ($V_{10}O_{28}^{6-}$) is the intercalated species in each case. Further data supporting this assertion have been presented elsewhere.[17] A broad peak in the PXRD pattern at low angle is present in both materials, although the position is variable (*ca.* 10.2 Å for MgAlV as synthesised and between *ca.* 8.8 and 10.4 Å for LiAlV samples). This peak may be tentatively assigned to a quasi-crystalline salt of Mg^{2+}/Al^{3+}/polyoxometalate ($MgAlCO_3$) or Li^+/Al^{3+}/polyoxometalate ($LiAlCO_3$). It is noted here, as previously,[31] that the development of the broad peak is independent of the nature of the metals in the cationic lattice, the nature of the polyoxometalate species and the synthesis conditions used to prepare the sample.

Differences in the thermal stability are not quite so marked in the vanadates as in the other inorganic intercalates. The MgAl material is more stable but dehydroxylation occurs over a wide range of temperatures between *ca.* 220 and 480 °C, whereas for the LiAl material the transition begins at *ca.* 300 °C and dehydroxylation is complete by 400 °C. Lopez Salinas and Ono[32] studied magnesium aluminium layered double hydroxides intercalated with decavanadate anions using infrared and powder X-ray diffraction, and studied the oxidation state of the vanadium species by EPR spectroscopy. They concluded that the $V_{10}O_{28}^{6-}$ breaks into smaller species at 200 °C, which rearrange to form polymeric vanadate species $[\text{-}VO_3\text{-}]_n^{n-}$ at 300–350 °C. The vanadium is gradually reduced from an oxidation state of V^V to V^{IV}. The layered structure remains intact, although the layers are completely dehydroxylated. At 400–450 °C, the brucite-like layers are transformed into magnesium aluminium oxide structures which react with the vanadate species at *ca.* 600 °C, forming crystalline α-$Mg_2V_2O_7$. Furthermore, Twu and Dutta[33] investigated the thermal properties of $LiAlV_2O_7$ LDHs using powder X-ray diffraction, diffuse reflectance and Raman spectroscopy. They concluded that the $V_2O_7^{4-}$ species dimerised in the interlayer at 80–100 °C to form $V_4O_{12}^{4-}$ and subsequently polymerised to give O-$(VO_2)_n$-O units at temperatures between 100 and 300 °C. Dehydroxylation of the layers occurs at 300–400 °C and the layered structure itself collapses above 450 °C to yield Li_3VO_4, $LiVO_3$ and Al_2O_3.

Hammett indicator tests

Hammett indicator tests (Fig. 1) show the carbonate containing LDHs to have strong basic sites of $pK_a > 12.2$, both before and after calcination for 2 h at 400 °C. This is in agreement with the findings of Nakatasuka *et al.*[34] who found basic sites of a range of strengths up to $18.0 \geqslant H_o \geqslant 17.2$. Tichit *et al.*[35] reported that $MgAlCO_3$ was more basic than pyridine ($pK_a = 8.8$) and of similar basicity to piperidine (11.12). Corma *et al.*[36] found that carbonate-intercalated LDHs contain basic sites with pK_a values in the range 10.7–13.3 and a few sites with pK_a of 16.5.

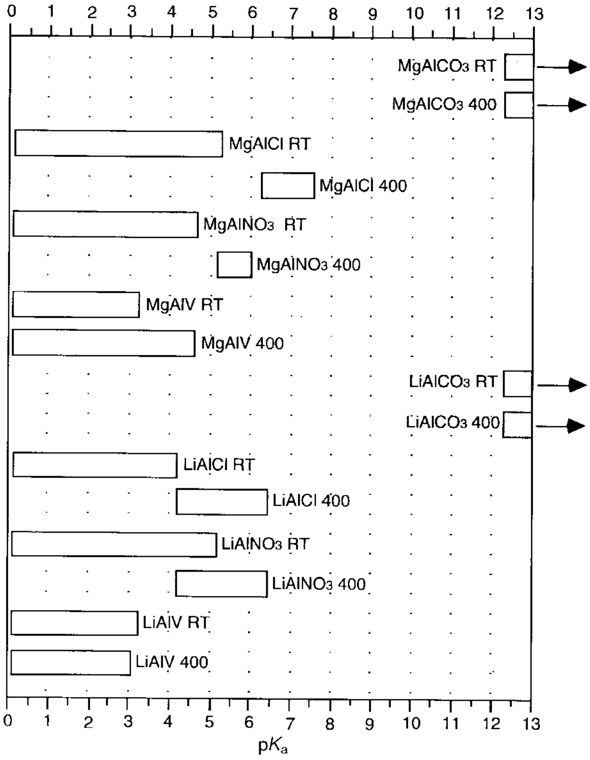

Fig. 1 pK_a values for the various LDHs and their calcination products, determined using Hammett indicators (numbers denote calcination temperatures, RT denotes an untreated sample)

The vanadate-intercalated materials, however, possess mainly sites of strength $0.1 \leqslant H_o \leqslant 3.2$, which are again independent of calcination temperature. These more acidic sites thus appear to be associated with the interlayer vanadate species rather than the LDH matrix itself.

The chloride and nitrate-intercalated samples, whether in a MgAl or LiAl matrix, display acidity somewhere in between those of the carbonate and vanadate systems. They are most acidic prior to calcination at 400 °C, with strength $0.1 \leqslant H_o \leqslant 5.2$ and more basic following calcination ($4.2 \leqslant H_o \leqslant 7.6$). Miyata[20] found that MgAlCl calcined at 500 °C possessed active sites of $H_o \leqslant 4.8$ and $H_o \leqslant 1.5$, and a small number of sites with $H_o \leqslant -3$.

It may thus be concluded that the identity of the interlayer anion is more influential with regard to the acidity or basicity of an LDH than the nature of the matrix itself. The reasons for this behaviour will be discussed subsequently.

Pyridine adsorption

The FTIR spectrum recorded for $MgAlCO_3$ treated at 250 °C after adsorption of pyridine shows broad, ill-defined bands. In the sample treated at 400 °C these bands are much stronger and well defined, at 1625 (shoulder), 1607, 1601, 1492 and 1448 cm^{-1}. All the bands[37,38] result from the vibrational modes ν_{8a}, ν_{19a}, ν_{19b} modes of co-ordinated pyridine, *i.e.* pyridine adsorbed on surface Lewis acid sites.[39] Similar bands have been described in the literature for pyridine adsorbed on alumina,[40] the first three bands have been ascribed to pyridine bonded to tetrahedral Al^{3+} sites (1625 cm^{-1}), pyridine adsorbed on a tetrahedral Al^{3+} site placed near a cationic vacancy (1607 cm^{-1}) and pyridine bonded to an octahedral Al^{3+} site (1601 cm^{-1}).[41,42]

$LiAlCO_3$, $LiAlNO_3$ and LiAlCl LDHs calcined at 250 or at 400 °C, give rise, upon adsorption of pyridine, to spectra with bands at 1586, 1576, 1450 and 1435 cm^{-1}. These bands are due to physisorbed pyridine, as they are easily removed after outgassing at room temperature. Thus, as the lithium is very basic it cancels the acidity created by the aluminium. A similar behaviour was observed for $MgAlNO_3$. After adsorption of pyridine, the spectra of $MgAlNO_3$, calcined at 250 and 400 °C, show bands at 1587, 1576, 1449 and 1433 cm^{-1}, due to physisorbed pyridine. These are removed when the samples are outgassed at temperatures lower than 100 °C, thus indicating the absence of surface acid sites.

By contrast, a MgAl sample containing vanadium treated at 250 °C shows a spectrum [Fig. 2(A)] with bands at 1605, 1597 (shoulder), 1576, 1489 and 1444 cm^{-1}, corresponding to pyridine coordinated to Lewis acid sites. Splitting of the band (1605 and 1597 cm^{-1}) due to the ν_{8a} mode indicates that two types of surface Lewis acid sites exist, corresponding to tetrahedral Al^{3+} sites placed near a cationic vacancy and octahedral Al^{3+} sites.[40,41] The first band could also be related to adsorption on coordinatively unsaturated V^{5+} sites (which can also act as Lewis acid sites).[43] Furthermore, the adsorption of pyridine on vanadia-containing systems is known to give rise to a band at 1605 cm^{-1}. The band at 1597 cm^{-1} could be ascribed to pyridine physisorbed or hydrogen-bonded to Mg^{2+} sites, as a band in the same position is recorded after adsorption of pyridine on MgO,[44] which is removed after outgassing at room temperature. However, in the present case the band is removed only after outgassing at 200 °C and so it may be better ascribed to pyridine adsorbed on weak Al^{3+} acid sites. The weak band recorded in the spectrum of MgAlV at 1538 cm^{-1} could be ascribed to the ν_{19b} mode of the pyridinium ion, thus suggesting formation of Brønsted acid sites, developed by the presence of vanadium.

The bands recorded after adsorption of pyridine on MgAlV treated at 400 °C [Fig. 2(B)] are better defined than those detected in the sample treated at 250 °C. The bands are recorded at 1605, 1597, 1488 and 1445 cm^{-1} (due to coordinated pyridine) and 1636 and 1538 cm^{-1}, due to the ν_{8a} and ν_{19b} modes of the pyridinium ion. In agreement with the findings for the previous sample, both Lewis and Brønsted sites exist, although in this case, the relative intensities of the bands suggest a larger concentration of Brønsted sites. Thus it may be concluded that an increase in the calcination temperature gives rise to an increase in surface acidity, favouring formation of Brønsted sites.

When the samples are outgassed at increasing temperatures (Fig. 2), a general decrease in the intensities of the bands due to both Lewis and Brønsted acid sites is observed for MgAlV previously calcined at either 250 or 400 °C. The band at 1597 cm^{-1} is removed when the sample is calcined at 200 °C. In order to remove all bands due to adsorbed pyridine, the sample has to be outgassed at 300 °C, thus indicating that the surface acid sites are relatively strong, probably coordinatively unsaturated Al^{III} and V^{V} sites. Furthermore, during outgassing, the bands are shifted towards higher wavenumbers, the ν_{8a} band shifting from 1605 to 1611 cm^{-1}, and the ν_{19b} band from 1445 to 1449 cm^{-1}.

Adsorption of pyridine on MgAlCl calcined at 250 °C and outgassed at room temperature gives rise to broad bands [Fig. 3(A)] at 1607, 1485 and 1445 cm^{-1}, due to adsorption on surface Lewis sites. Weak bands at 1635 and 1530 cm^{-1} are due to the pyridinium ion, *i.e.* showing the presence of Brønsted acid sites. However, both the Brønsted and Lewis bands are removed when the sample is outgassed at 250 °C which suggests that these acid sites are relatively weak. For the sample calcined at 400 °C [Fig. 3(B)], the bands due to pyridine coordinated to surface Lewis acid sites are stronger and better defined, and are recorded at 1607, 1601(shoulder), 1491, 1447 and 1441 cm^{-1}. Splitting of the band due to the ν_{8a} mode (to bands at 1607 and 1601 cm^{-1}) is similar to that described above for $MgAlCO_3$ and MgAlV and is due to the presence of weak Lewis acid sites with different strengths. However, the bands at 1635 and 1530 cm^{-1}, observed for MgAlCl treated at 250 °C and due to protonated pyridine, are virtually absent in this sample. Thus it may be concluded that MgAlCl shows a surface Brønsted acidity similar to that for MgAlV, although these sites are destroyed at 400 °C. The bands at 1601 and 1441 cm^{-1} are readily removed when the sample is outgassed at increasing temperatures.

In the case of the LiAl series of compounds, adsorption of pyridine is observed only on LiAlV calcined at 250 °C; for other vanadium-containing samples only a weak adsorption due to physisorbed pyridine is observed, and all bands are removed when the samples are outgassed at room temperature. The spectrum for LiAlV calcined at 250 °C is very similar to that recorded for alumina. Three bands are recorded at 1625, 1613 and 1597 cm^{-1}, as described for $MgAlCO_3$. As with MgAlV, the band recorded at 1597 cm^{-1} may also be ascribed to pyridine coordinated to weak Lewis acid sites (coordinatively unsaturated Li^+ species), as a band in a similar position has been recorded in the spectrum of Li/TiO_2 and MoO_3/TiO_2 doped with alkali metal metal cations.[45,46] It should be noted that no band could be ascribed to protonated pyridine, *i.e.* Brønsted acid sites do not exist on this sample. Nevertheless,

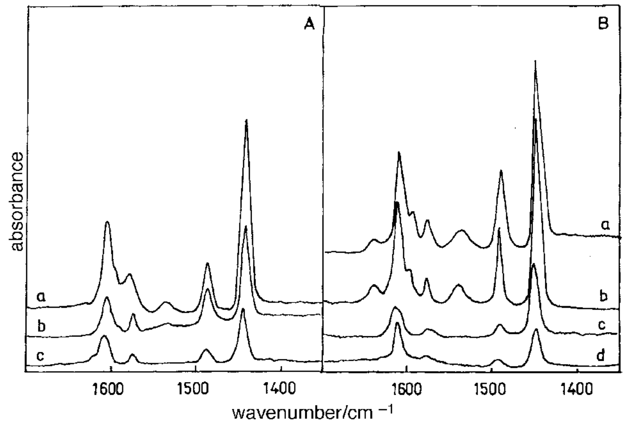

Fig. 2 IR spectra recorded after adsorption of pyridine at room temperature on samples (A) MgAlV/250, (B) MgAlV/400 and outgassing at (a) r.t., (b) 100, (c) 200 and (d) 300 °C

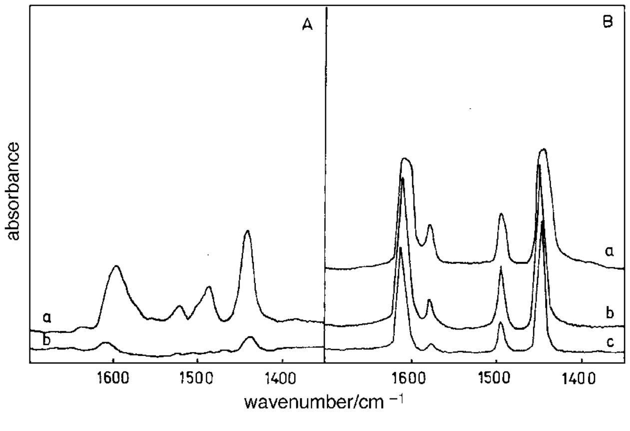

Fig. 3 IR spectra recorded after adsorption of pyridine at room temperature on samples (A) MgAlCl/250, (B) MgAlCl/400 and outgassing at (a) r.t., (b) 100 and (c) 200 °C

the surface acid sites are rather weak, as all bands are removed when the sample is outgassed above 250 °C.

It is well known that doping systems with cations or anions can modify the surface acidity/basicity.[45–48] In the present case, incorporation of vanadium in MgAl and LiAl LDHs result in the development of surface Lewis and/or Brønsted acidity (the latter only on MgAl samples); such centres are observed in MgAlCl but not in $MgAlNO_3$. Several theoretical models have been described in the literature to explain changes in the surface acidity after the addition of doping species. Tanabe[15] assumes that the generation of acidic centres is dependent on the charge in excess in the cation: if the excess is positive, Lewis centres are generated, but if it is negative, Brønsted sites develop. Connell and Dumesic[49] explain the development of Lewis sites, after doping of silica with metal cations, assuming that the formal charge on the cation is balanced by surface coordination of lattice oxide anions. The doping cation will behave as a Lewis site (*i.e.* coordinatively unsaturated) if the coordination number is lower than that for the cation existing in the undoped solid. On the other hand, the strength of Lewis acid sites depends on the electronegativity of the metal cations. In the present case, Li^+, Mg^{2+}, Al^{3+} and V^{5+} may behave as Lewis sites, their strength increasing in the order $Li < Mg < Al < V$. The existence of Lewis sites (Al^{3+}) in LiAlV (absent in $LiAlCO_3$) can be explained on the basis of the coexistence of Li and V giving rise to the formation of either amorphous or crystalline V–Li–O compounds, depending on the Li : V ratio. Such sites have been detected in V_2O_5/TiO_2 systems doped with alkali metal cations;[45] in this way, the surface Lewis acid sites (Al^{3+}) are not removed.

Generation of Brønsted sites can proceed *via* addition of water vapour (thus removing Lewis sites, as in the case of zeolites or alumina), or by formation of bridging hydroxyl groups due to the interaction of different phases. In the case of the vanadium-containing samples, development of Brønsted sites can be readily explained as V–OH moieties (*i.e.* Brønsted acid sites) exist on vanadate or polyvanadate species. However, formation of Brønsted acid sites in MgAlCl may be explained by a different mechanism; in this case (as in those systems containing P, F, S, *etc.*), the presence of electronegative anions could give rise to anionic Brønsted sites, different from those previously mentioned. Ghosh and Kydd[50] suggest that a weakening of the O—H bond occurs due to an inductive effect of the electronegative anions, while Kiselev and Krylov[51] assume that adsorption of water on electronegative anions leads to the formation of weak O—H bonds that behave as Brønsted acid sites.

The increase in the concentration of surface Brønsted acid sites for MgAlV as the calcination temperature is increased can be explained by assuming a breakdown of the lattice, thus leading to formation of crystalline V_2O_5 which possesses Brønsted acid sites. However, a larger concentration of Brønsted acid sites is observed for MgAlCl calcined at 250 °C; according to Miyata[20] total removal of chloride is attained only after calcination at 450–480 °C, and so larger amounts of chloride in the low temperature calcined samples would account for the larger concentration of Brønsted acid sites.

Isopropanol adsorption

The spectroscopic behaviour with regard to isopropanol adsorption is very similar for $MgAlCO_3$, $MgAlNO_3$ and all the LiAl samples. The spectra for sample LiAlV calcined at 400 °C is shown in Fig. 4(A). The main bands are recorded at 1471 [$\delta_{as}(CH_3)$], 1457, 1387 [$\delta_s(CH_3)$], 1156, 1136, 1094 and 1075 cm^{-1}, and show formation of isopropoxide, as a result of dissociative isopropanol adsorption.[39] A band at 1255 cm^{-1} could be ascribed to physisorbed isopropanol, or isopropanol hydrogen-bonded to surface basic sites[52] [the δ(O–H) band is recorded at 1252 cm^{-1} for monomeric isopropanol]. Other bands at 1630 and 3500–3000 cm^{-1} are due to δ(O–H) and ν(O–H) of molecular water. As the temperature is increased, no significant change is observed in these bands, while two new bands develop at 1734 ± 4 and 1720 ± 3 cm^{-1} when the sample is heated to 300 °C. These bands may be due to ν(C=O) of acetone either physisorbed or weakly coordinated to weak surface Lewis sites. Also, the bands at 1212 and 1234 cm^{-1} are due to ν(C–C–C) of acetone; this band is recorded at 1215 cm^{-1} for gaseous acetone. The intensities of these bands slightly increase when the sample is heated to 400 °C, while new bands develop at 1580 cm^{-1} (LiAl samples) or 1469 cm^{-1} ($MgAlNO_3$ and $MgAlCO_3$ samples). This band can be tentatively ascribed to ν_{as}(COO) of the carboxylate species; the corresponding ν_s(COO) band is not evident, as it would be obscured by the bands of isopropoxy not participating in the oxidative dehydrogenation to acetone; its position should be close to 1449 cm^{-1}.

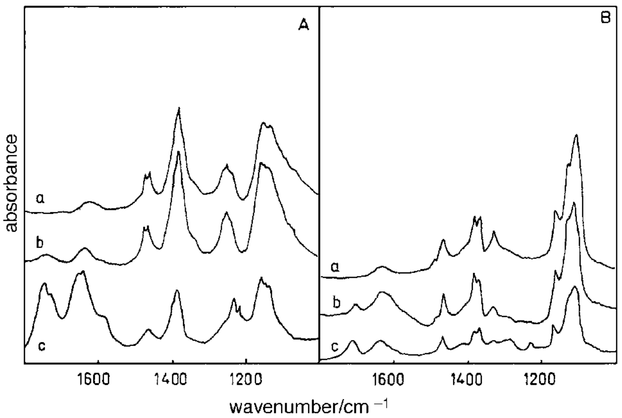

Fig. 4 IR spectra recorded after adsorption of isopropanol on samples (A) LiAlV/400, (B) MgAlV/400 and outgassing at (a) r.t., (b) 300 and (c) 400 °C

The spectra recorded for MgAlCl and MgAlV after adsorption of isopropanol [Fig. 4(B)] are also rather similar. Bands are recorded at 1486, 1466, 1383, 1368, 1330, 1168, 1130 and 1110 cm^{-1}. The bands are mostly due to the isopropoxy species, resulting from the dissociative adsorption of isopropanol. The band at 1630 cm^{-1} is due to δ(O–H) of molecular water. (Contrary to the behaviour observed for the $MgAlCO_3$, $MgAlNO_3$ and the LiAl series of samples, there is no evidence for molecular adsorption of isopropanol, nor physisorbed, nor hydrogen-bonded to basic centres, nor isopropanol coordinated to Lewis acid sites.) When MgAlV is heated to 300 °C, a new band is recorded at 1700 cm^{-1}, of greater intensity than that observed in MgAlCl and can be ascribed to ν(C=O) of acetone coordinated through the oxygen atom to Lewis acid sites. This band is recorded at lower wavenumber than in samples described above, thus confirming the greater strength of the acid sites which exist in these samples. As above, however, the ν(C–C–C) band (more intense than for MgAlCl) is recorded at 1234 cm^{-1}.

The oxidative properties and surface basicities of the solids prepared can be concluded from the isopropanol adsorption studies. The results show that adsorption follows similar trends to those previously described by several authors.[52–55] In all samples, the following has been observed: (i) dissociative adsorption of isopropanol, leading to formation of the isopropoxy species and water (bands at 1630 and 3500–3000 cm^{-1} due to $\delta_{O\text{–}H}$ and $\nu_{O\text{–}H}$). The presence of these species indicates that adsorption has taken place in the form:

$$(CH_3)_2CHOH + L^{n+}_{(s)} + OH^- \rightarrow (CH_3)_2CHO^- \text{---} L^{n+}_{(s)} + H_2O$$

(ii) molecularly adsorbed isopropanol, only in the less acidic samples (LiAl, $MgAlCO_3$ and $MgAlNO_3$).

Oxidation of the alkoxide to acetone (isopropanol dehydrogenation) takes place in all cases at high temperature (300–400 °C). As surface basic sites are required for such a dehydrogenation to account for proton abstraction, as opposed to dehydration (requiring surface acid sites) leading to propene, we can conclude that basic sites exist in all samples studied here. However, their quantification is not possible using this technique. Nevertheless, it may be concluded that MgAlCl samples and those containing vanadium show a larger surface acidity, as well as stronger acid sites. As acetone is strongly held to the surface Lewis acid sites, the $\nu(C{=}O)$ band shifts towards lower wavenumber and acetone is largely retained when the sample is outgassed. Also, formation of acetate species (as detected for LiAl samples, $MgAlCO_3$ and $MgAlNO_3$) after adsorption of isopropanol indicates a larger nucleophilic character for these samples, where molecular isopropanol adsorbed on basic sites has also been observed.

Catalysis

A. Acetaldehyde self-condensation. Aldol condensation reactions may be used to synthesise a wide variety of organic compounds. Laboratory scale catalysts which have been used include alumina,[56,57] aluminium *tert*-butoxide,[58] zeolites[59] and sepiolites.[60] On a larger scale, alkali and alkaline earth metal hydroxides and a range of acids, bases and transition metal complexes have been used.[13,61–64]

The self-condensation of acetaldehyde may be catalysed by both Lewis or Brønsted sites of basic character. In the first step two molecules of acetaldehyde undergo addition to form 3-hydroxybutanal. In the presence of strongly basic catalysts (*i.e.* with basic sites of $pK_a > 11.2$)[65] the 3-hydroxybutanal will dehydrate to form crotonaldehyde—crotonaldehyde is, however, an important solvent and precursor chemical and is hence the desired product. Crotonaldehyde itself may be converted to an enolate anion by reaction with a further basic site and through repeated addition and dehydration polymeric products may be formed (C_6, C_8, *etc.*).

Fig. 5(a) shows the total conversion of acetaldehyde obtained for $MgAlCO_3$ and MgAlV materials treated at a range of temperatures, plotted against the selectivity towards crotonaldehyde (at a reaction temperature of 110 °C). The activity of MgAlV is affected greatly by calcination temperature, with conversion of 19.6% for a non-calcined sample, rising to a maximum of 44.2% conversion for a sample calcined at 450 °C and decreasing after calcination at 600 °C to 31.2%. Thus it may be concluded that basic sites are generated at higher temperature and/or there is an increase in the accessible surface area for catalysis. Selectivity to crotonaldehyde is inversely proportional to activity, as the production of polymeric products is proportionately greater for the more active catalysts.

$MgAlCO_3$ exhibits activity of between 27.2 and 33.0%, depending on calcination temperature. Unlike the case for MgAlV the activity is not greatly affected by thermal pretreatment of the catalyst. Thus it may be concluded that $MgAlCO_3$ possesses a similar number and strength of basic sites irrespective of calcination temperature. The selectivity to crotonaldehyde is significantly lower than that of MgAlV.

The behaviour of LiAlV [Fig. 5(b)] is similar to that of its MgAl analogue with respect to this reaction, although the reactivity of the LiAl material is uniformly higher and the selectivity is uniformly lower. Once again, maximum catalytic activity is obtained for a sample calcined at 450 °C. This is in agreement with many literature studies which generally conclude that maximum base-catalytic activity for hydrotalcite-like materials is obtained following calcination at *ca.* 450 °C and the subsequent dehydration and dehydroxylation.[66–69]

$LiAlCO_3$ LDHs are found to be less active than $MgAlCO_3$ LDHs, regardless of calcination temperature. This would suggest that they are less basic. Maximum activity is obtained after 400 °C calcination for $LiAlCO_3$. The lithium materials are once again found to exhibit higher selectivity towards crotonaldehyde than their MgAl analogues.

Substitution of chloride or nitrate anions for carbonate [Fig. 6(a)] yields an improvement in product selectivity but little change in activity for MgAl samples. For the LiAl system, substitution leads to materials with decreased activity and improved selectivity.

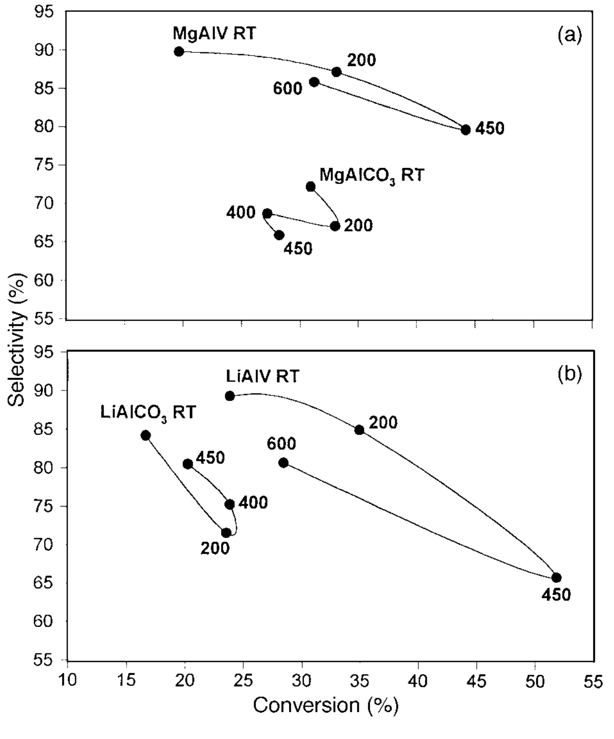

Fig. 5 Conversion of acetaldehyde against selectivity to crotonaldehyde for (a) MgAl LDHs and (b) LiAl LDHs catalysing the self-condensation of acetaldehyde (reaction temperature 112 °C; numbers denote calcination temperature of catalyst)

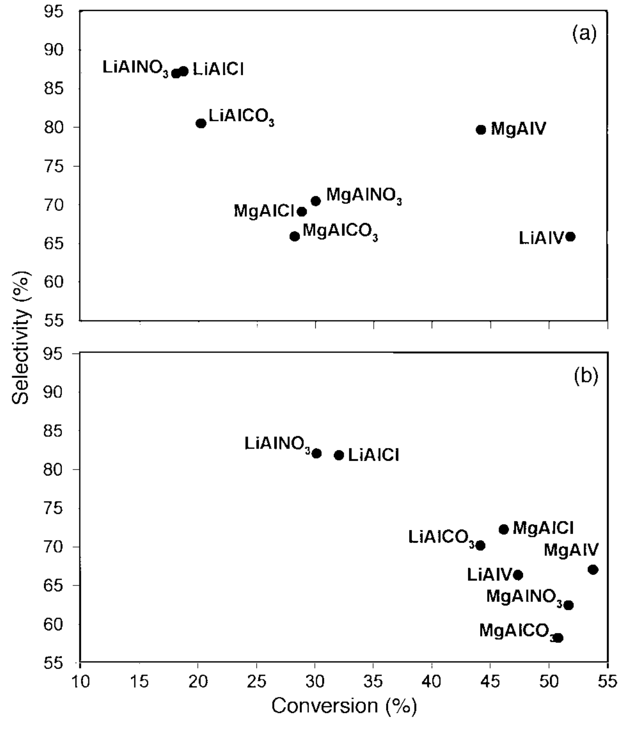

Fig. 6 Conversion of acetaldehyde against selectivity to crotonaldehyde for LDHs catalysing the self-condensation of acetaldehyde at (a) 112 °C, (b) 124 °C (calcination temperature of catalysts 450 °C)

When the reaction temperature was increased from 112 to 124 °C, in all samples except LiAlV activity was increased [Fig. 6(b)]. This is in agreement with the work of Kagunya,[70] who found that maximum catalytic activity for this reaction increased up to a temperature of 120 °C but decreased with further increase in temperature. Here, for most of the catalysts the increase in activity is obtained at the expense of selectivity. Indeed, it was found that generally selectivity to crotonaldehyde was inversely related to activity.

The observed order of reactivity is $LiAlNO_3 < LiAlCl < LiAlCO_3 < MgAlCO_3 \approx MgAlCl \approx MgAlNO_3 < MgAlV < LiAlV$. With the exception of the vanadate intercalates, it would appear that the MgAl matrix has enhanced basic properties compared to the LiAl system. This may be attributed to the presence of Mg–O Lewis base sites on the MgAl materials. The reason for the increased basicity of the vanadate samples, and in particular the large increase in activity observed for LiAlV over other LiAl systems is not fully understood.

B. 2-Methylbut-3-yn-2-ol conversion. 2-Methylbut-3-yn-2-ol (MBOH), the simplest tertiary alkynol, is a highly polar molecule which is soluble in water. It gives different products when reacting on acidic, basic or amphoteric materials.[71] On acid sites, dehydration to yield 3-methylbut-3-en-1-yne (Mbyne) occurs, whereas base-catalysed cleavage results in the formation of acetone and acetylene. By-products such as 3-hydroxy-3-methylbutan-2-one (HMB) and the corresponding dehydrated product, 3-methylbut-3-en-2-one (MIPK) may be formed in the presence of amphoteric catalysts.

$MgAlCO_3$ displays a high level of activity for MBOH conversion, and the highly basic selectivity of this material is demonstrated by the fact that acetone and acetylene were the only reaction products formed up to a reaction temperature of 250 °C [Fig. 7(a)]. Thus it may be concluded that the reaction occurs almost wholly on basic sites. Constantino and Pinnavaia[18] proposed that the basic guest anions participate in the catalytic reaction through interaction with the reagent at the external basal and edge surfaces of the layers.

$LiAlCO_3$ demonstrates a higher catalytic ability for this reaction, with *ca.* 75% conversion at a reaction temperature of 150 °C and almost total conversion at higher temperatures. In this case, some acidic character is detected, with *ca.* 18% of the conversion proceeding by the acidic pathway at 300 °C [Fig. 7(b)].

The behaviour of the vanadate-intercalated materials is markedly different, however. MgAlV is significantly less active for MBOH conversion than the carbonate LDHs, with conversion of <15% at 150 °C and <35% at 300 °C [Fig. 8(a)]. Here, only minor amounts of acetone and acetylene are produced, and the reaction proceeds mainly *via* an acid-catalysed pathway to yield Mbyne as the major product. Significant quantities of HMB and MIPK are also produced, suggesting a degree of amphoteric character is present in this sample.

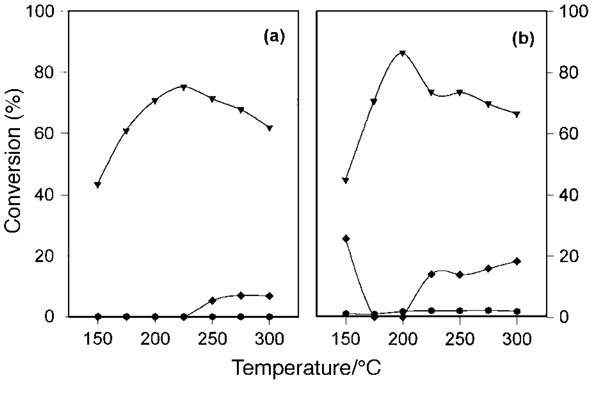

Fig. 7 Product distribution for MBOH conversion using (a) $MgAlCO_3$ and (b) $LiAlCO_3$ catalysts; (▼) basic; (◆) acidic; (●) amphoteric activity

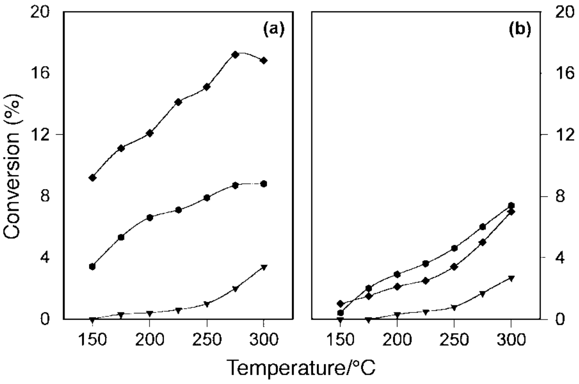

Fig. 8 Product distribution for MBOH conversion using (a) MgAlV and (b) LiAlV catalysts; (▼) basic; (◆) acidic; (●) amphoteric activity

LiAlV is the least active catalyst for this reaction, with only *ca.* 20% conversion at a temperature of 300 °C. As for MgAlV, there is little basic selectivity; rather most of the activity occurs *via* acidic and amphoteric pathways, with roughly equal proportions of each of the products [Fig. 8(b)].

Finally, MgAlCl was used as a catalyst for MBOH conversion. It was expected on the basis of the results described previously that it would display activity and selectivity between those of the carbonates and vanadates. Indeed, this was found to be the case; conversions of between *ca.* 25 and 75% were achieved, depending on reaction temperature, and although the reaction proceeded mainly by the acidic pathway, significant basic character was observed. This is in agreement with the work of Constantino and Pinnavaia,[18] who found that although all crystalline LDH intercalates displayed high basic selectivity, the oxides obtained from the thermal decomposition of chloride and sulfate intercalated LDHs exhibited acidic sites in addition to basic centres. They proposed that in the case of the chloride materials, the acidity could arise from the replacement of hydroxyl groups in the brucite-like layers by the chloride anion.

On the basis of the results described above, it may be concluded that MBOH is a highly sensitive probe for determining the acid/base selectivity of LDHs. The anion greatly influences the LDH reactivity, as witnessed by the fact that carbonate activity > chloride > decavanadate.

Conclusions

Effect of the host matrix

The host matrix was not found to have a dominant effect on either the acidity or catalytic activity of the LDHs, although the enhanced thermal stability of the MgAl materials is clearly desirable.

Effect of calcination temperature

It is generally agreed that calcination temperature has a large effect on the catalytic performance of LDHs. Reichle[61] found a maximum in catalytic activity and selectivity at a calcination temperature of between 400 and 450 °C. Untreated hydrotalcite was reported to be catalytically inactive. Tichit *et al.*[69] also reported that activity increased with calcination temperature. In contrast, Constantino and Pinnavaia[18] reported that crystalline LDHs were more active for 2-methylbut-3-yn-2-ol decomposition than the amorphous oxides produced following calcination. The untreated samples were also more active than the crystalline spinel phases formed following calcination at

900 °C. They suggested that the lower activity of the amorphous oxides was due to the collapse of the charged layers. Our results are generally in agreement with those of the former authors. In the case of vanadate-intercalated materials in particular, calcination at *ca.* 400 °C leads to a material of high activity. Catalysis using LiAlV LDHs has been performed by Twu and Dutta,[33] who proposed that in order to provide access to the interlayer vanadium sites it is necessary to partially destroy the framework by thermal decomposition.[66,72,73] They suggest that a catalytically active $O(\text{-}VO_2\text{-})_nO$ layer is generated at 350–450 °C. Our results confirm that vanadate-intercalated layered double hydroxides are precursors to materials with high catalytic activity following calcination at *ca.* 400–450 °C.

Effect of the interlayer anion

Reichle[61] concluded in his early studies of the catalytic performance of LDHs that the identity of the interlayer anion had a large effect on the catalytic performance of the materials. He reported that calcination of $MgAlCO_3$ yields a highly active catalyst upon calcination at 450 °C. However, in the case of sulfates, halides, chromates, *etc.* the elimination of the anion cannot take place at this temperature; rather, the anion is irreversibly bound to the mixed oxide matrix in place of the catalytically effective hydroxyl group. Such materials would be catalytically inactive. Suzuki and Ono[74] also reported that carbonates are the most active catalysts in several reactions.

The phenomenon of grafting of anions to the cationic matrix has been subsequently reported by other authors. Constantino and Pinnavaia[18] reported that oxides formed from the decomposition of MgAlCl possess acidic as well as basic sites. They proposed that this was due to chloride grafting. The activity of uncalcined LDH catalysts was largely influenced by anion basicity; thus $MgAlCO_3$ and MgAlOH were more active for 2-methylbut-3-yn-2-ol conversion than MgAlCl. When MgAlCl was in an anhydrous state (following treatment at 150–250 °C) it functioned as a base catalyst. At 350 °C there was a decrease in activity and acidic character was generated which was explained by chloride grafting. Some hydroxyl groups are bound to metal centres adjacent to halide ions. Cl–M–OH subunits may function as Brønsted acid sites due to the electron withdrawing effect of the chloride ions.

Our results show the catalytic activity of layered double hydroxides to be greatly affected by the nature of the interlayer anion. More acidic anions lead to catalysts with higher acidic functionality. Thus the catalytic activity for acid catalysed reactions increases in the order carbonate < nitrate < chloride < vanadate.

We gratefully acknowledge the support of the Engineering and Physical Sciences Research Council (studentship to I.C.C.). This work was carried out under the framework of the Concerted European Action on Pillared Layered Solids (CEA-PLS), with financial support from Junta de Castilla y Leon (Consejeria de Educaciou y Cultura, grant SA45/96).

References

1 T. W. Bastock and J. H. Clark, in *Speciality Chemicals*, Elsevier Science Publishers, Amsterdam, 1991.
2 *Preparative Chemistry using Supported Reagents*, ed. P. Laszlo, Academic Press, London, 1987.
3 *Solid Supports and Catalysts in Organic Synthesis*, ed. K. Smith, Ellis Horwood, Chichester, 1992.
4 J. H. Clark, A. P. Kybett and D. J. Macquarrie, *Supported Reagents: Preparation, Analysis and Applications*, VCH, Weinheim, 1992.
5 P. E. Hathway and M. E. Davis, *J. Catal.*, 1989, **116**, 263.
6 H. Scheper, J. J. Berg-Slot and W. H. J. Stork, *Appl. Catal.*, 1989, **54**, 79.
7 H. Knözinger, H. Bühl and K. Kochloefl, *J. Catal.*, 1972, **24**, 57.
8 E. J. Rode, P. E. Gee, L. N. Marquez and T. Uemura, *Prepr. ACS Symp. Ser.*, 1989, **34**, 467.
9 D. Barthomeuf, G. Coudurier and J. C. Vedrine, *Mater. Chem. Phys.*, 1988, **18**, 553.
10 A. Auroux and J. C. Vedrine, in *Catalysis by Acids and Bases*, ed. B. Imelik, C. Naccache, G. Coudurier, Y. Ben Taarit and J. C. Vedrine, Elsevier Science Publishers, Amsterdam, 1985.
11 W. Hölderich, M. Hesse and F. Naumann, *Angew. Chem., Int. Ed. Engl.*, 1988, **27**, 226.
12 A. Corma, R. M. Martín-Aranda and F. Sánchez, *J. Catal.*, 1990, **126**, 192.
13 F. Cavani, F. Trifirò and A. Vaccari, *Catal. Today*, 1991, **11**, 173.
14 H. A. Benesi and B. H. C. Winsquist, *Adv. Catal.*, 1978, **27**, 98.
15 K. Tanabe, *Solid Acids and Bases, Their Catalytic Applications*, Academic Press, London, 1970, in *Catalysis Sciences and Technology*, ed. J. R. Anderson and M. Bondart, Springer-Verlag, Berlin, 1981, vol. 2, p. 231.
16 J. Kijenski and A. Baiker, *Catal. Today*, 1989, **5**, 1.
17 I. C. Chisem and W. Jones, *J. Mater. Chem.*, 1994, **4**, 1737.
18 V. R. L. Constantino and T. J. Pinnavaia, *Inorg. Chem.*, 1995, **34**, 883.
19 I. C. Chisem, S. D. Cosgrove and W. Jones, *J. Thermal Anal.*, 1997, **50**, 757.
20 S. Miyata, *Clays Clay Miner.*, 1975, **23**, 369.
21 J. Shen, J. M. Kobe, Y. Chen and J. A. Dumesic, *Langmuir*, 1994, **10**, 3908.
22 W. T. Reichle, *Solid State Ionics*, 1986, **22**, 135.
23 A. L. McKenzie, C. T. Fishel and R. J. Davis, *J. Catal.*, 1992, **138**, 547.
24 M. J. Hernandez, M. A. Ulibarri, J. Cornejo, M. J. Peña and C. J. Serna, *Thermochim. Acta*, 1985, **94**, 257.
25 M. J. Hernandez, M. A. Ulibarri, J. L. Rendon and C. J. Serna, *Thermochim. Acta,* 1984, **81**, 311.
26 O. Marino and G. Mascolo, in *2nd Eur. Symp. on Thermal Analysis*, Aberdeen, 1981, ed. D. Dollimore, Heyden, London, 1981, p. 391.
27 G. W. Brindley and S. Kikkawa, *Clays Clay Miner.*, 1980, **28**, 87.
28 A. Clearfield, M. Jieke, J. Kwan, J. L. Colon and R. C. Wang, *J. Inclusion Phenom. Mol. Recognit. Chem.*, 1991, **11**, 361.
29 J. R. Butruille, L. J. Michot, O. Barrés and T. J. Pinnavaia, *J. Catal.*, 1993, **139**, 664.
30 M. J. Hernandez-Moreno, M. A. Ulibarri, J. L. Rendon and C. J. Serna, *Phys. Chem. Miner.*, 1985, **12**, 34.
31 F. Kooli, V. Rives and M. A. Ulibarri, *Inorg. Chem.*, 1995, **34**, 5114.
32 E. Lopez Salinas and Y. Ono, *Bull. Chem. Soc. Jpn.*, 1992, **65**, 2465.
33 J. Twu and P. K. Dutta, *J. Phys. Chem.*, 1989, **93**, 7863.
34 T. Nakatsuka, H. Kawasaki, S. Yamashita and S. Kohjiya, *Bull. Chem. Soc. Jpn.*, 1979, **52**, 2449.
35 D. Tichit, M. H. Lhouty, A. Guida, B. H. Chiche, F. Figueras, A. Auroux, D. Bartalini and E. Garrone, *J. Catal.*, 1995, **151**, 50.
36 A. Corma, V. Fornés, R. M. Martin-Aranda and F. Rey, *J. Catal.*, 1992, **134**, 58.
37 E. P. Parry, *J. Catal.*, 1963, **2**, 371.
38 E. B. Wilson, *Phys. Rev.*, 1934, **45**, 706.
39 L. J. Bellamy, *The Infra-red Spectra of Complex Molecules*, Chapman and Hall, London, 1975.
40 C. Martín, I. Martín, V. Rives, S. Damyanova and A. Spojakina, *React. Kinet. Catal. Lett.*, 1995, **54**, 203.
41 C. Morterra, A. Chiorino, G. Ghiotti and E. Garrone, *J. Chem. Soc., Faraday Trans. 1*, 1979, **75**, 271.
42 G. Busca, V. Lorenzelli and V. S. Escribano, *Chem. Mater.*, 1992, **4**, 595.
43 C. Martín, V. Rives and D. Klissurski, *XIV Iberoamerican Symposium on Catalysis*, Concepción, Chile, 1994.
44 C. Martín, I. Martín and V. Rives, *J. Mol. Catal.*, 1992, **73**, 51.
45 G. Busca and G. Ramis, *Appl. Surf. Sci.*, 1986, **27**, 114.
46 C. Martín, I. Martín, C. del Moral and V. Rives, *J. Catal.*, 1994, **146**, 415.
47 G. Connell and J. A. Dumesic, *J. Catal.*, 1987, **105**, 285.
48 C. Martín, I. Martín, V. Rives, L. Palmisano and M. Schiavello, M., *J. Catal.*, 1992, **134**, 434.
49 G. Connell and J. A. Dumesic, *J. Catal.*, 1986, **102**, 216.
50 A. K. Ghosh and R. A. Kydd, *Catal. Rev. Sci. Eng.*, 1985, **27**, 1569.
51 V. F. Kiselev and O. V. Krylov, *Adsorption Processes on Semiconductor and Dielectric Surface I*, Springer Series in Chemical Physics, ed. R. Gomer, Springer-Verlag, Berlin, 1985, p. 32.
52 P. F. Rossi, G. Busca, V. Lorenzelli, O. Saur and J. C. Lavalley, *Langmuir*, 1987, **3**, 52.
53 K. Buckman, B. Grzybowska, M. Che and J. M. Tatibuet, *Appl. Catal. A – General*, 1993, **96**, 279.
54 G. Ramis, G. Busca and V. Lorenzelli, *J. Chem. Soc., Faraday Trans. I*, 1987, **83**, 1591.

55 G. A. M. Hussein, N. Sheppard, M. I. Zaki and R. B. Fahin, *J. Chem. Soc.*, *Faraday Trans. 1*, 1989, **83**, 1723.

56 J. Muzart, *Synthesis*, 1982, **1**, 60.

57 J. Muzart, *Synth. Commun.*, 1985, **15**, 285.

58 M. Jerry, *Advanced Organic Chemistry*, 4th edn., John Wiley and Sons, Chichester, 1992, p. 938.

59 A. Corma and R. M. Martin-Aranda, *J. Catal.*, 1991, **130**, 130.

60 A. Corma, V. Fornes, R. M. Martin-Aranda, H. Garcia and J. Primo, *Appl. Catal.*, 1990, **59**, 237.

61 W. T. Reichle, *J. Catal.*, 1980, **63**, 295.

62 N. B. Lorrette, *J. Org. Chem.*, 1957, **22**, 346.

63 D. Walther and E. Dinjus, *Z. Anorg. Allg. Chem.*, 1978, **440**, 22.

64 M. J. Astle and J. A. Zaslowsky, *Ind. Eng. Chem.*, 1952, **44**, 2867.

65 G. Zhang, H. Hattori and K. Tanabe, *Appl. Catal.*, 1988, **36**, 189.

66 W. T. Reichle, *J. Catal.*, 1985, **94**, 547.

67 C. P. Kelkar, A. Schutz and G. Marcelin, *Perspectives in Molecular Sieve Science*, ed. W. H. Flank and T. E. White, University Pittsburgh, 1988, p. 324.

68 M. Chibwe, Ph.D. Thesis, University of Cambridge, 1990.

69 D. Tichit, M. H. Lhouty, A. Guida, B. H. Chiche, F. Figueras, A. Auroux, D. Bartalini and E. Garrone, *J. Catal.*, 1995, **151**, 50.

70 W. Kagunya, PhD. Thesis, University of Cambridge, 1992.

71 H. Lauron-Pernot, F. Luck and J. M. Popa, *Appl. Catal.*, 1991, **78**, 213.

72 C. Busetto, G. Del Piero and G. Manara, *J. Catal.*, 1984, **85**, 260.

73 W. T. Reichle, S. Y. Kung and D. S. Everhardt, *J. Catal.*, 1986, **101**, 352.

74 E. Suzuki and Y. Ono, *Bull. Chem. Soc. Jpn.*, 1988, **61**, 1008.

Paper 8/01323C; *Received* 16*th February*, 1998